

Spectrally Resolved Chemiluminescent Probes for Sensitive Multiplex Molecular Quantification

Kenneth A. Browne,^{*,†} Dimitri D. Deheyn,[‡] Richard C. Brown,^{§,||} and Ian Weeks^{§,⊥}

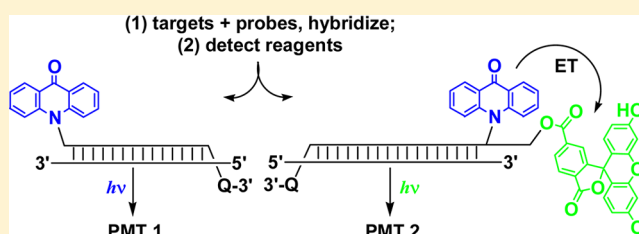
[†]Gen-Probe Incorporated, 10210 Genetic Center Drive, San Diego, California 92121, United States

[‡]Marine Biology Research Division, Scripps Institution of Oceanography, University of California at San Diego, La Jolla, California 92093, United States

[§]Molecular Light Technology Research Ltd. (now Gen-Probe Life Sciences Ltd., Crewe Road, The Oaks Business Park, Wythenshawe, Manchester M23 9HZ, U.K.).

S Supporting Information

ABSTRACT: Luminophores are frequently utilized probe labels for detecting biological analytes. Multiple fluorescent luminophores, or fluorophores, can be readily distinguished from one another based on different energy excitation and emission wavelengths and lifetimes. However, suitable methods and reagents for distinguishing multiples of the much more sensitive chemically initiated luminophores have been limited. Herein we describe a new class of hybrid luminophore probes that emit light of distinct wavelength ranges and intensities upon energy transfer (ET) from an in-common, acridinium ester chemiluminophore to a covalently conjugated fluorophore. This format supports rapid, rational design of spectrally resolvable, chemically initiated probes. Time-resolved spectrographic and luminescence characterizations indicate that ET is not dependent on overlap in the emission spectrum of the luminophore and the absorption spectra of acceptors, suggesting a non-Förster resonance ET mechanism. Analysis of a combination of the chemiluminophore and new chemiluminophore-acceptor conjugate probes demonstrates the benefits of their use in sensitive, multiplex quantification of nucleic acid sequences indicative of environmentally relevant microbes without prior enzymatic amplification.



Hybridization of nucleic acid probes to complementary nucleic acid targets has been critical to the development of rapid molecular detection of specific sequences^{1–4} in fields ranging from clinical diagnostics to forensics and environmental monitoring. Sensitive probe labels evolved from radioisotopes^{1,2} to chemiluminophores³ and fluorophores,³ and discrimination of bound from unbound probes improved from heterogeneous formats^{1,2} (requiring substantial washing of hybridized sequences to remove unhybridized probe) to an increased reliance on homogeneous formats^{3,4} that do not require such steps. Detection of high concentrations (e.g., high nanomolar) of multiple nucleic acid targets through implementation of molecular beacons (MBs) and related fluorescent probe technologies^{3,5} has increased the value of homogeneous assays in terms of information returned, cost, and time, especially if preceded by amplification of the target sequence. MBs function as homogeneous probes by their ability to change secondary structure and, thus, modulate signaling activity. Self-complementary nucleotide (nt) sequences near each terminus of MBs promote a stem-loop structure that constrains the fluorophore (F) at one terminus to the proximity of a quenching moiety at the opposite terminus, leading to low emission of light upon excitation of the fluorophore in the absence of target. Hybridization of a complementary target to the loop sequence forces the stem sequences as well as the fluorophore and quencher

apart, thereby signaling the presence of a specific target through increased detectable fluorescence.

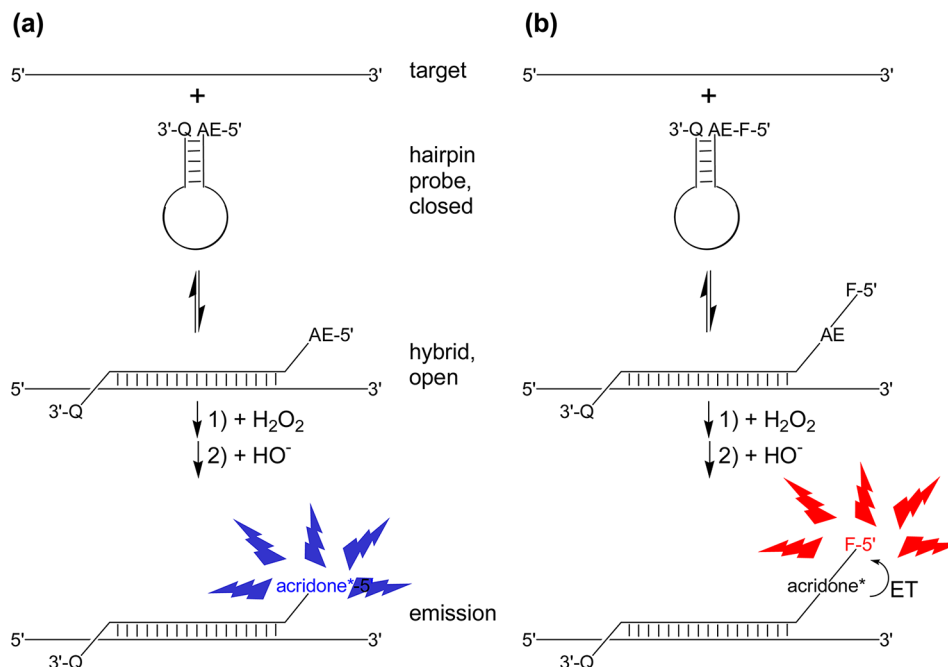
Excitation light and nonspecific fluorescence in a sample contribute to background fluorescence, while these sources of background are absent in chemiluminescent systems. Lower background signals from a chemically initiated (rather than from a photonicly initiated), electronically excited state molecule allow detection of emissions to be much more sensitive than by fluorescence. Acridinium ester (AE) probes, for example, exhibit the ability to homogeneously report low concentrations (down to high picomolar) of complementary target over a wide dynamic range in the presence of closely related targets.⁴ Light from chemiluminescent reactions has traditionally been collected over entire luminophore emission ranges (within the limits of the detector), reducing the number of co-occurring targets that can be simultaneously quantified. The current work tests a rational design hypothesis to facilitate rapid generation of many chemiluminescent probes with different wavelength emissions by solid phase oligonucleotide synthesis, biophysical evaluation of these wavelength-shifted (ws) probes, and demonstration of these probes' utility in multiple analyte detection.

Received: July 13, 2012

Accepted: September 28, 2012

Published: October 22, 2012



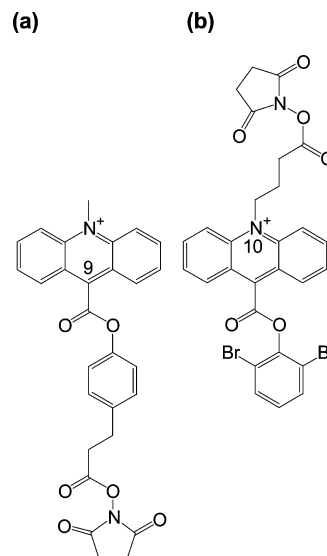
Scheme 1. (a) HICS and (b) wsHICS Probe Reactions^a

^aHybridization of a HICS probe loop to a complementary target nucleic acid forces the stem arms and, hence, the quenching moiety (Q) and the luminophore (a) AE or (b) AE-fluorophore (AE-F) construct apart. Addition of oxidizing agent and increased alkalinity initiates light emission characteristic of (a) the electronically excited species (acridone*) or (b) the F after ET from the acridone*. In the absence of target, the stem arms remain hybridized, Q and the luminophore remain proximal, and little energy as light emissions is detected. Solid lines between nucleic acid strands represent base pairing.

RESULTS

Design. Hybridization-induced chemiluminescent signal (HICS) probes have been described recently.^{6,7} These probes comprise structures similar to MBs except that they possess an AE chemiluminophore instead of a fluorophore attached to the terminus opposite the quenching moiety (Scheme 1a). An important aspect of their design is the use of an AE label attached to the probe sequence through the N10 position of the acridinium rather than through groups linked to the C9 position (Chart 1); this enables the excited 10-alkyl-9(10*H*)-acridone (*N*-alkylacridone*) to remain attached to the probe sequence and in proximity to other chromophores on the same probe sequence during detection.⁸ A further design characteristic is the facilitation of rapid chemiluminescence initiation at a sufficiently low pH (≤ 9) to maintain hybridization between the probe arms or between the probe loop region and the target in the absence or presence of complementary target sequence, respectively. This has been previously studied in terms of the reduction of the leaving group pK_a through substitution of the phenoxy group.^{9–11} Not only did the low pK_a of the diortho-bromo substitution (~ 6.4 ; cf $pK_a \sim 9.9$ and 10.6 for unsubstituted phenol and 2,6-dimethylphenol, respectively) increase the rate of chemiluminescence emission compared to the unsubstituted phenol under the same detection conditions,^{9,10} but the steric hindrance of this substitution also increased the hydrolysis storage stability relative to the unsubstituted phenol.¹⁰ An important stability aspect of the reagent formulation for assays using HICS probes includes use of a low pH buffer and surfactant in the hybridization reagent to provide conditions that protect the acridinium esters from hydrolysis and nonspecific adsorption and nucleic acids from nucleases. Additionally, inclusion of an appropriate surfactant

Chart 1. Structures of (a) C-Linked and (b) N-Linked AE NHS Ester Label Compounds



enhances the chemiluminescence yield from the luminophore of acridinium esters.^{12,13} Excitation of different emitter fluorophores by a single type of nearby harvester fluorophore species has been demonstrated with MBs complementary to different target sequences.⁵ Chemical initiation of a single type of AE label on a HICS probe (analogous to a harvester fluorophore) could provide sufficient energy to transfer to different proximally attached emitter fluorophores, enabling light emission at wavelengths distinct from AE itself (Scheme 1b). A series of HICS and wsHICS probes and their complementary target sequences (Table 1) were synthesized to test this hypothesis.

Table 1. Probe and Target Sequences

name ^a	nucleic acid backbone ^b	sequence ^c
<i>EfaB874-888(-)</i> HICS1	DNA	5'-AE-TGCGTG CTCAATTCGAGGCT CACGCA-D-3'
<i>EfaB874-888(-)</i> wsHICS10a	DNA	5'-FAM-AE-TGCGTG CTCAATTCGAGGCT CACGCA-D-3'
<i>EfaB874-888(-)</i> wsHICS10b	DNA	5'-AE-FAM-TGCGTG CTCAATTCGAGGCT CACGCA-D-3'
<i>EfaB874-888(-)</i> wsHICS11a	DNA	5'-TAM-AE-TGCGTG CTCAATTCGAGGCT CACGCA-D-3'
<i>EfaB874-888(-)</i> wsHICS12a	DNA	5'-Cy5-AE-TGCGTG CTCAATTCGAGGCT CACGCA-D-3'
<i>EfaB874-888(-)</i> wsHICS20a	DNA	5'-FAM-T-AE-TGCGTG CTCAATTCGAGGCT CACGCA-D-3'
<i>EfaB866-896(+)</i>	DNA	3'-GGTAGTAA GAGTTAAGGCTCCGA TCGGGATT-5'
		890 880 870
<i>EcoB1932-1947(-)</i> HICS18	OMe/DNA	5'-AE-CCCAGCAC CGACAAGGAAUUUCGC GTGCTGGG-BHQ2-3'
<i>EcoB1921-1958(+)</i>	RNA	3'-GCCUUGAAUGG GCUGUCCUUAAGCG AUGGAAUCCUG-5'
		1950 1940 1930
<i>CalA1185-1206(-)</i> wsHICS88	DNA	5'-TAM-AE-CCGAGGAC GTCTGGACCTGGTGAAGTTTCCC GTCCTCGG-D-3'
<i>CalA1174-1217(+)</i>	RNA	3'-GGAAUAAACA CAGACUGGACCAUCUAAAGG GCACAACUCAG-5'
		1210 1200 1190 1180
<i>CtrB1452-1465(+)</i> HICS51	OMe	5'-AE-CCGAC AGAGCGAUGAGAAC GUCGG-BHQ2-3'
<i>CtrB1447-1470(-)</i>	OMe	5'-C-3'-3'-AGGCA UCUCGCUACUCUUG CCAAU-5'
		1450 1460 1470
<i>NgoA133-145(+)</i> wsHICS63	OMe	5'-TAM-AE- CCGAG GUACCGGGUAGCG CUCGG-D-3'
<i>NgoA128-150(-)</i>	OMe	5'-C-3'-3'-CCUUG CAUGGCCCAUCGC CCCC-5'
		130 140 150

^aTarget and corresponding probe names derived from the three letter abbreviations (Genus species) of the reference sequences, a letter indicating the small (A) or large (B) rRNA subunit, the target sequence range and an internally derived unique designation for the probes (e.g., HICS1). *Efa* sequences are Enterococcus specific probes and targets to/from the *Enterococcus faecalis* 23S rRNA reference sequence (NCBI Accession No. AJ295306); *Eco* sequences are pan-bacterial probes and targets to/from the *Escherichia coli* O157:H7 23S rRNA reference sequence (NCBI Accession No. E16366); *Cal* sequences are pan-fungal probes and targets to/from the *Candida albicans* 18S rRNA reference sequence (NCBI Accession No. E15168); *Ctr* and *Ngo* sequences are probes and targets to/from Transcription-Mediated Amplification amplicon sequences of *Chlamydia trachomatis* 23S rRNA (NCBI Accession No. AM884176) and *Neisseria gonorrhoeae* 16S rRNA (NCBI Accession No. NC_002946), respectively. Target names are given in bold characters. Numbering to reference targets indicated underneath each class of reference sequences. ^bBackbone sugar structures of probe and target nucleic acids: DNA, deoxyribose (underlined); RNA, ribose; OMe, 2'-methoxyribose. ^c"AE" signifies the position of an N-linked AE chemiluminophore label on an amine linker. "FAM," "TAM," and "Cy5" denote the attached fluorophores 6-carboxyfluorescein, 5- (and 6-)carboxytetramethylrhodamine and cyanine dye 5 labels, respectively. "D" and "BHQ2" indicate the attachment location of the quenching moieties dabcyI and Black Hole Quencher-2.

Predictable Spectral Emissions. Spectrography was used to record time-resolved spectrograms of chemiluminescence and ET from AE to nearby fluorophores of a series of HICS and wsHICS probes with the same sequence but differing in fluorophore acceptor or its position. In the absence of an attached fluorophore, time-resolved chemiluminescence spectrograms of *EfaB874-888(-)*HICS1 plus complementary target quickly increased to a peak before decaying over about 20 s (Figure 1a). The sequential spectrograms clearly show emissions in the 400–520 nm wavelength range and double peaks at ~425 and ~448 nm that are characteristic of *N*-alkylacridone* fluorescence emission.¹⁴ In the absence of target (Figure 1a, inset), chemiluminescence was similar to that from hybridization reagent alone (data not shown), demonstrating efficient quenching. Chemiluminescence from *EfaB874-888(-)*wsHICS10a plus target also quickly rose to a peak before decreasing over ~10 s (Figure 1b). Emission wavelengths ranged from ~490–600 nm with a maximum at ~520 nm, consistent with fluorescein fluorophore emission and suggesting efficient ET from *N*-alkylacridone* to the fluorophore. Chemiluminescence from *EfaB874-888(-)*wsHICS11a plus target quickly peaked before slowly decaying over at least 60 s (Figure 1c); emissions ranged from ~540–670 nm with a maximum at ~580 nm, as expected from the tetramethylrhodamine

fluorophore and again supporting efficient ET from *N*-alkylacridone* to the fluorophore despite little overlap in *N*-alkylacridone* emission and tetramethylrhodamine absorption bands (~460–590 nm). Chemiluminescence from *EfaB874-888(-)*wsHICS12a plus target quickly increased to a peak but then slowly decayed over more than 120 s (Figure 1d). Wavelength emissions ranged from ~600–790 nm with a maximum at ~680 nm, consistent with Cy5 fluorophore emissions (except with an additional peak/shoulder at ~750 nm), supporting efficient ET from *N*-alkylacridone* to the fluorophore even though there was essentially no overlap between *N*-alkylacridone* emission and Cy5 absorption wavelengths (~520–690 nm). Unlike *EfaB874-888(-)*wsHICS10a and *EfaB874-888(-)*wsHICS11a, *EfaB874-888(-)*wsHICS12a in the absence of target sequence yields a small but detectable background emission (Figure 1d, inset). This is consistent with the relative quenching efficiencies of these dyes by dabcyI;¹⁵ using an alternate quenching moiety such as BHQ2 with more uniform quenching efficiencies among these fluorophores would be expected to largely ameliorate background signals. The uniform chemiluminescence rise and fall across spectrograms in each example is supportive of detectable emission from single species (*N*-alkylacridone*, or fluorescein, tetramethylrhodamine or Cy5 fluorophores). These results demonstrate

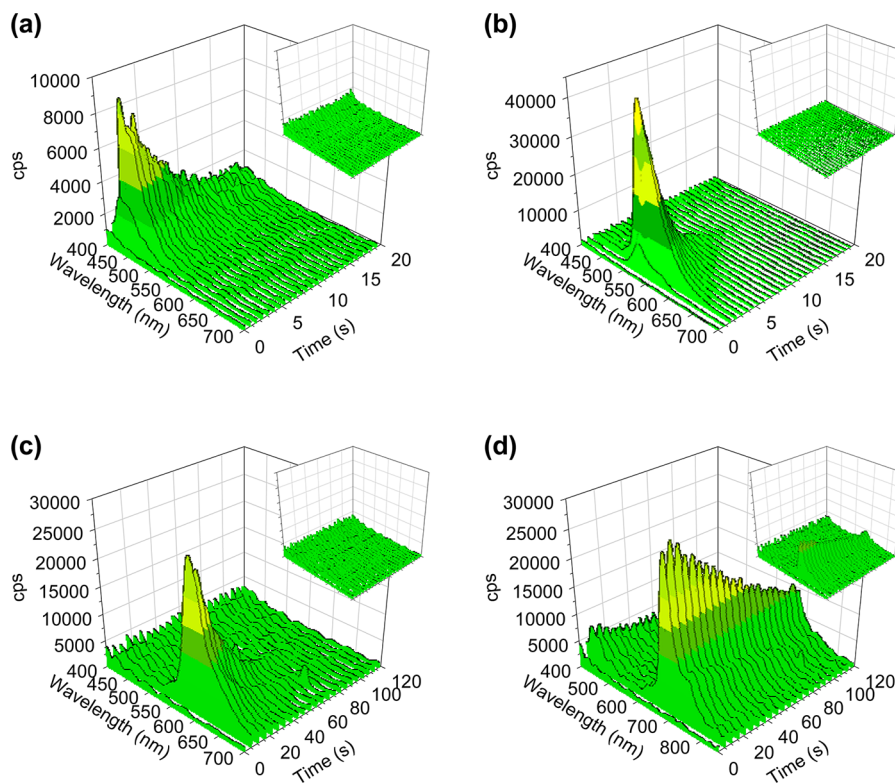


Figure 1. Probe emissions. Time-resolved spectrograms of cps summed over the preceding 0.4 s interval (a and b) or the preceding 5 s interval (c and d) after chemical initiation of (a) 50 pmol *EfaB874-888(-)HICS1*, (b) 100 pmol *EfaB874-888(-)wsHICS10a* (AE-fluorescein), (c) 50 pmol *EfaB874-888(-)wsHICS11a* (AE-tetramethylrhodamine), and (d) 200 pmol *EfaB874-888(-)wsHICS12a* (AE-Cy5) prehybridized to equimolar amounts of their complementary targets in hybridization reagent; insets show results for probes in the absence of target with the same axis scales. Color patterns in graphs are to better distinguish signal magnitudes and consecutive spectrograms.

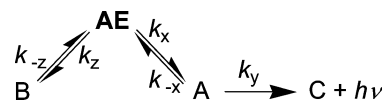
principles to design distinct wsHICS probes based on fluorophore emission characteristics but without the criterion of overlapping chemiluminophore donor emission and fluorophore acceptor absorption wavelengths.

Quantitative Emission Characteristics. Time-resolved, total wavelength luminescence emissions of HICS and wsHICS probes complementary to different targets and with different nucleic acid backbones (Table 1) were plotted as summed counts per second (cps) versus time (Figure S1 in the Supporting Information). The emissions increased to a peak and then decreased toward zero. As observed previously for chemiluminescent reactions proceeding through an acridone*,^{8,16} two apparent first-order, competing and parallel reactions most simply account for the formation and decay of chemiluminescent emissions. This allowed data fitting to a linear combination of exponential equations (eq 1) based on a kinetic scheme

$$\text{cps} = a(-\exp^{-k_a t}) + b(\exp^{-k_b t}) \quad (1)$$

(Scheme 2) simplified from one that includes a series of more elementary steps.⁸ (A related but alternate set of reaction pathways leading to chemiluminescence from 10-methyl-9-(phenoxycarbonyl)acridinium salts was recently detailed.¹⁷ An important distinction is decomposition of a 1,2-dioxetane intermediate into an *N*-alkylacridone* and the release of a proposed phenyl carbonate rather than a previously proposed phenolate and CO₂. Distinguishing between these pathways is beyond the scope of the current studies and does not change the currently used simplified kinetic scheme.) These optimized fits yielded physical constants that quantitatively defined each of the probes (Table 2), and cps versus time values back-calculated from eq 1 and the

Scheme 2. Kinetic Scheme for Minimum Reaction Events Supporting Observed Luminescent Emissions from AEs



physical constants closely followed the observed data points regardless of whether the reaction sequence included ET or not. Rates of increase in cps up to maximum intensity were rapid with $\tau_{1/2,a} < 500$ ms, and they varied $< \sim 3$ -fold among all probes. Rates of subsequent intensity decrease were much slower and more variable with $\tau_{1/2,b}$ ranging up to nearly 25 s and varying > 30 -fold among all probes. Rate constants for intensity decreases were similar for related chemiluminophores or chemiluminophore-fluorophore conjugates regardless of the nucleic acid backbones comprising the probes, varying up to ~ 3 -fold among the three HICS probes (*EfaB874-888(-)HICS1*, *EcoB1932-1947(-)HICS18*, and *CtrB1452-1465(+HICS51)*), the three wsHICS AE-fluorescein probes (*EfaB874-888(-)wsHICS10a*, *EfaB874-888(-)wsHICS10b*, and *EfaB874-888(-)wsHICS20a*) or the three wsHICS AE-tetramethylrhodamine probes (*EfaB874-888(-)wsHICS11a*, *CalA1185-1206(-)wsHICS88*, and *NgoA133-145(+wsHICS63)*). In this sense, k_b were better descriptors of the different probe and probe labels than k_a . When tested (*EfaB* probe series), total emission and wavelength-resolved emission intensities yielded formation or decay constants similar to within ~ 2 -fold, supporting that the observed total luminescence was primarily due to the wavelength specific emissions. The position of the fluorophore impacted k_a or k_b by a factor of < 2 -fold for identical sequences

Table 2. Chemiluminescent Emission Constants for Probes^a

name	time-to-peak (s)	k_a (s ⁻¹) ^b	k_b (s ⁻¹) ^b	SA ^c (Σcps/pmol)	S/B ^c
<i>EfaB874-888(-)HICS1</i> ^d	0.55 [6]	4.66 ± 0.18 [10]	0.532 ± 0.017 [10]	(2.99 ± 0.14) × 10 ⁷ [10]	11.1 ± 0.5 [10]
<i>EfaB874-888(-)wsHICS10a</i> ^d	0.58 [4]	3.07 ± 0.16 [4]	0.785 ± 0.085 [10]	(5.23 ± 0.31) × 10 ⁷ [10]	22.1 ± 1.2 [10]
<i>EfaB874-888(-)wsHICS10a</i> ^e	0.84 [4]	1.89 ± 0.11 [4]	0.813 ± 0.022 [4]	(7.05 ± 0.39) × 10 ⁶ [4]	22.8 ± 1.1 [4]
<i>EfaB874-888(-)wsHICS10b</i> ^d	0.72 [4]	3.34 ± 0.19 [4]	0.441 ± 0.009 [12]	(4.65 ± 0.26) × 10 ⁷ [12]	17.0 ± 0.9 [12]
<i>EfaB874-888(-)wsHICS10b</i> ^e	0.78 [4]	3.02 ± 0.23 [4]	0.460 ± 0.007 [4]	(7.09 ± 0.16) × 10 ⁶ [4]	20.6 ± 0.7 [4]
<i>EfaB874-888(-)wsHICS11a</i> ^d	1.05 [6]	4.21 ± 0.31 [6]	0.0878 ± 0.0035 [8]	(2.10 ± 0.09) × 10 ⁷ [8]	5.08 ± 0.18 [8]
<i>EfaB874-888(-)wsHICS11a</i> ^e	1.35 [6]	3.12 ± 0.08 [6]	0.0661 ± 0.0017 [6]	(1.30 ± 0.06) × 10 ⁷ [6]	5.14 ± 0.25 [6]
<i>EfaB874-888(-)wsHICS20a</i> ^d	0.75 [6]	2.44 ± 0.06 [6]	0.713 ± 0.025 [12]	(5.09 ± 0.19) × 10 ⁷ [12]	13.9 ± 0.4 [12]
<i>EfaB874-888(-)wsHICS20a</i> ^e	1.12 [4]	1.43 ± 0.02 [4]	0.687 ± 0.012 [4]	(5.86 ± 0.24) × 10 ⁶ [4]	25.6 ± 0.9 [4]
<i>EcoB1932-1947(-)HICS18</i> ^{d,f}	0.70	3.99	0.291	3.34 × 10 ⁸	285
<i>CalA1185-1206(-)wsHICS88</i> ^d	0.98 [20]	5.69 ± 0.55 [17]	0.0343 ± 0.0011 [17]	(9.17 ± 0.58) × 10 ⁷ [17]	14.0 ± 0.8 [17]
<i>CtrB1452-1465(+)HICS51</i> ^{d,f}	0.75	2.11	0.924	1.72 × 10 ⁸	276
<i>NgA133-145(+)wsHICS63</i> ^d	0.97 [14]	4.92 ± 0.25 [4]	0.0283 ± 0.0006 [14]	(7.68 ± 0.19) × 10 ⁷ [14]	15.7 ± 0.5 [14]

^aSequences are in Table 1. Values are mean ± 1 standard deviation from chemical initiation of 0.5 pmol probe hybridized to 1 pmol complementary target in hybridization reagent. Brackets enclose the number of replicates. ^b k_a and k_b are from nonlinear best fits to eq 1 from at least 5 × first order half-lives ($\tau_{1/2}$) of each constant. ^cSpecific activities (SA) are from cps summed over 5 × $\tau_{1/2}$ of the decay process divided by the picomoles of probe, while signal-to-background ratios (S/B) are from cps summed over 5 × $\tau_{1/2}$ of the decay process for probe-target hybrids divided by the same sum for probes alone. ^dFrom light emission detected by PMT without being filtered. ^eFrom light emission detected by PMT after being filtered to >550 nm, specific for emission from ET acceptor. ^fPreviously reported.⁸

in which fluorescein is 5' of AE (*EfaB874-888(-)wsHICS10a*), AE is 5' of fluorescein (*EfaB874-888(-)wsHICS10b*), or fluorescein is 5' and one nt removed from AE (*EfaB874-888(-)wsHICS20a*), indicating tolerance of fluorophore acceptor location.

Specific activities (SAs) were similar (e.g., ~2–5 × 10⁷ Σcps/pmol) for *EfaB874-888(-)HICS1*–*EfaB874-888(-)wsHICS20a* despite a nearly 10-fold variation in the emission decrease rate constants of chemiluminescent emissions (0.088–0.81 s⁻¹). SAs decreased with increasing shift of emissions to wavelengths higher than those of the fluorescein-containing probes due, at least in part, to decreasing PMT efficiency at higher wavelengths (approaching zero above 650 nm in the current instrument); this efficiency decrease was sufficient to support only minimal detection of emissions from a Cy5 fluorophore (e.g., *EfaB874-888(-)wsHICS12a*, S/B approaching 1, data not shown). However, the SA for the AE-fluorescein conjugate probes (*EfaB874-888(-)wsHICS10a*, *EfaB874-888(-)wsHICS10b*, and *EfaB874-888(-)wsHICS20a*) were slightly higher than for the AE probe (*EfaB874-888(-)HICS1*) in the same series, suggesting that AE ET to fluorescein may advantageously enhance signal output relative to that of AE alone; this boost is tentatively assigned to the high quantum yield of fluorescein.

Wavelength-resolved SA varied by up to ~7-fold compared to total SA, likely largely due to a combination of ET and PMT filtering efficiencies. The SA and S/B tended to be lower for the all DNA probes than for the 2'-O-methylribonucleic acid or mixed backbone probes, though sequence context was not taken into account in this assessment. The position of the fluorophore impacted SA and S/B < 2-fold for identical sequences in which fluorescein is 5' of AE, AE is 5' of fluorescein, or fluorescein is 5' and one nt removed from AE. This finding supports continued use of the synthetically straightforward 3'-quencher-oligonucleotide-AE-fluorophore-5' probe design. All configurations of AE to fluorophore tested thus far maintain distances between these two moieties substantially closer than the optimal 7–9 nt previously cited for fluorophore-to-fluorophore ET.¹⁸

Spectral-Temporal Quantification of Multiple Sequences. Chemiluminescence measured with a dual wavelength luminometer demonstrated simultaneous, direct detection of bacterial and fungal rRNA sequences in seawater as simulated

indicators of bacteria and fungi quantities in a near shore oceanic environment (Figure 2). The tetramethylrhodamine label for the pan-fungal probe was selected from wsHICS probe characteristics (based on work with the *EfaB* probe series) that were spectrally distinguishable from the pan-bacterial HICS probe while yielding substantial S/B (Figure 1, Table 2). There was some spectral overlap from high concentrations of the wsHICS probe–target hybrid in the low wavelength channel and vice versa. To mitigate this overlap, differences in decay kinetics of the two probes were advantageously weighted by summing early time points from the rapidly emitting HICS probe signal in the low wavelength channel while summing the remaining later time points in the high wavelength channel for the slower emitting wsHICS probe, resulting in spectral-temporal resolution of the signals. Chemiluminescence from a mixture of *EcoB1932-1947(-)HICS18* and *CalA1185-1206(-)wsHICS88* in solutions containing equal volumes of hybridization reagent and seawater increased after hybridization to increasing concentrations of *Eco* or *Cal* rRNA sequences. In the absence or presence of the *Cal* target, curves for increasing *Eco* target in the low wavelength channel increased linearly from ~2–200 fmol, with the lower end of the range limited by signals from bleed-through of very high concentrations of *Cal* target (Figure 2a). Maintaining the *Eco* target constant at 50 fmol and increasing *Cal* target from 0.2–200 fmol yielded a line of zero slope, essentially the same as if no *Cal* target had been added. *Cal* target yielded similar quantitative dynamic range and limit of detection results in the high wavelength channel (Figure 2b). Thus, sequences from either or both pan-generic targets could be simultaneously quantified from ~2–200 fmol in a 50 μL sample within about 60 min.

DISCUSSION

The present study provides an improved route to rapid synthesis of sensitive, wavelength-distinguishable, chemiluminescent probe sets that can be individually detected and quantified simultaneously after a chemical initiation step. Chemiluminescent outputs from several wavelengths have been successfully achieved based on ET from a chemiluminophore to different fluorophores covalently linked at various distances from the

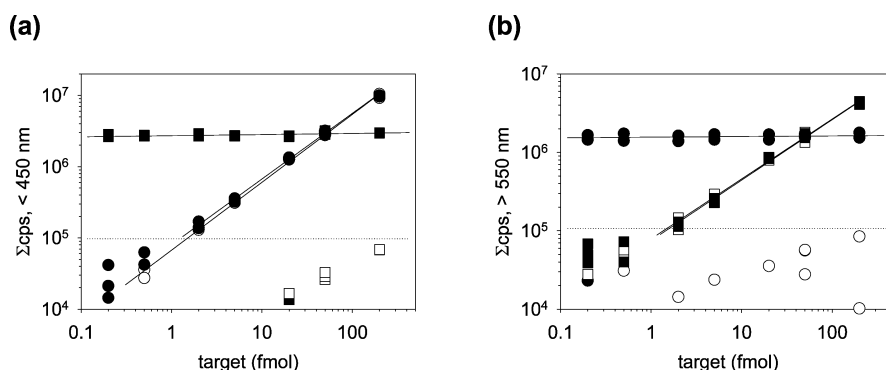


Figure 2. Chemiluminescent quantification curves. Background subtracted emissions from 200 fmol of both *EcoB1932-1947(-)*HICS18 and *CalA1185-1206(-)*wsHICS88 probes versus synthetic *EcoB1921-1958(+)* (○) and *CalA1174-1217(+)* (□) target concentrations in equal volumes of seawater and hybridization reagent; open symbols (○, □) are in the presence of indicated target, closed symbols (●, ■) are in the presence of indicated target plus 50 fmol of the other target. Points in (a) show the short wavelength-resolved cps summed from 0–12 s ($5 \times \tau_{1/2}$ of *EcoB1932-1947(-)*HICS18), and points in (b) show the long wavelength-resolved cps summed from 12–101 s (after $5 \times \tau_{1/2}$ of *EcoB1932-1947(-)*HICS18 through $5 \times \tau_{1/2}$ of *CalA1185-1206(-)*wsHICS88). All conditions were performed in at least duplicate. Solid lines through increasing data points are linear best fits {Table S1 in the Supporting Information}. Solid lines through horizontal data points are linear best fits to 50 fmol specific target in the presence of increasing (as indicated on *x*-axis) nonspecific target (slope <0.021 in all cases). The dotted lines intersect with the solid target-response at the minimum of one target that can be distinguished in the presence of 200 fmol of the other target.

chemiluminophore, with emissions defined and characteristic of the fluorophores only, thus permitting rational design of probe labels for multiplex end-point molecular assays. The self-quenching nature of these nucleic acid probes in the absence of complementary target ensures they are amenable to homogeneous hybridization assays for detection and/or quantification of any desired target.

The predictable changes of emission wavelengths, and substantial emission kinetics and quenching changes, from wsHICS probes relative to HICS probes (Figure 1, Table 2) provide insight into the mechanism of chemically initiated ET to fluorophores. If ET and/or excited fluorophore decay is fast compared to *N*-alkylacridone* decay (and at 10^9 s^{-1} , the latter is certainly true), k_b will be dependent on *N*-alkylacridone* decay rate and will therefore be similar for all probes. Using ET to fluorescein (*EfaB874-888(-)*wsHICS10a, *EfaB874-888(-)*wsHICS10b, and *EfaB874-888(-)*wsHICS20a) as an example motif is consistent with this supposition as k_b for these probes differed less than ~50% from that of *EfaB874-888(-)*wsHICS1. However, k_b values from AE-tetramethylrhodamine conjugates (e.g., *EfaB874-888(-)*wsHICS11a, *CalA1185-1206(-)*wsHICS88, and *NgoA133-145(+)*wsHICS63) were much lower (~6- to 32-fold) than directly from *N*-alkylacridone* of similar nucleic acid backbone probes (e.g., *EfaB874-888(-)*HICS1, *EcoB1932-1947(-)*HICS18, and *CtrB1452-1465(+)*HICS51). If fluorophore wavelength emission depends on overlap between the *N*-alkylacridone* emission spectrum and fluorophore excitation spectra (resonance ET), longer wavelength fluorophores should yield substantially decreasing emission intensity. However, as the spectrograms demonstrate, total emission from wsHICS probes was high, even when the overlap integral between the donor emission and the acceptor absorption spectra is near zero (Figure 1a versus Figure 1d). In the absence of target, ET to the quenching moieties can be, at the very least, from the *N*-alkylacridone* (Figure 1a) but may also be from the fluorophores (e.g., Figure 1d, inset). If the quenching moieties capture energy from the primary emitter, then quenching should be similar for HICS and wsHICS probes (especially within a series of identical sequences). As evidenced by background time-resolved spectrograms and S/B, probes without fluorophores

(e.g., *EfaB874-888(-)*HICS1, *EcoB1932-1947(-)*HICS18, and *CtrB1452-1465(+)*HICS51) quench emissions more efficiently than probes that include tetramethylrhodamine near the *N*-alkylacridone* (e.g., *EfaB874-888(-)*wsHICS11a, *CalA1185-1206(-)*wsHICS88, and *NgoA133-145(+)*wsHICS63). Overall, these results support that at least some of the fluorophores are excited from the *N*-alkylacridone* by a radiationless mechanism other than Förster-type resonance ET and that dabcyI and BHQ2 quench wsHICS emissions from the fluorophores rather than from the *N*-alkylacridone*; additional studies are needed to identify the ET mechanism.

Various methods have been developed to permit the simultaneous detection of more than one target using chemi- or bioluminescence. For example, in a multistep, two protein analyte, heterogeneous assay, Adamczyk et al. stimulated an aequorin label with Ca^{2+} , recorded the luminescence, and then initiated and recorded luminescence from an acridinium-9-carboxamide label with alkaline peroxide.¹⁹ Previously, we demonstrated that two analyte nucleic acids could be homogeneously and simultaneously quantified down to 0.5–5 fmol by using a pair of HICS probes with distinct AE labels (either AE or 2,7-dimethoxyAE) and independently detecting either low or high wavelength emissions, respectively.⁸ However, considerable effort is involved in the synthesis of new AE labels for probes with differentiable spectral characteristics (compared to using a single type of AE label with nearby fluorescent acceptors as probes), thereby reducing throughput for design, synthesis, and screening of large numbers of wavelength-distinguishable chemiluminescent probes.

Examples of ET from chemiluminophores to fluorophores have been reported for analyte detection, mostly as intermolecular combinations. Patel and Campbell used chemiluminescence ET from aminobutylethyl-isoluminol-labeled haptens to fluorescein-labeled antibodies to quantify small molecules in serum or tissues.²⁰ Heller and Morrison designed pairs of nucleic acid probes labeled with luminol or rhodamine at their termini such that only upon hybridization of both probes to a complementary sequence would the chemiluminophore and the fluorophore be proximal, capable of ET and reporting of the analyte.²¹ Schaap et al. reported enzymatic triggering of a dioxetane substrate resulting in ET to a fluorescein conjugate

embedded in a cetyltrimethylammonium bromide micelle, leading to a 400-fold increase in detected light compared to that from the dioxetane alone.²² In a heterogeneous assay, Zhang et al. used binary nucleic acid probes labeled with luminol and a fluorophore (but fluorescein instead of rhodamine) and a third unlabeled probe to bind to an aptamer sequence and signal the presence of a bound ATP molecule.²³ Slightly different from the above examples, Soukka et al. disclosed a system in which electrochemiluminescence energy is transferred to a fluorophore acceptor and the emitted radiation detected.²⁴ Departing from the above works, and of the intramolecular nature of the present probes, the disclosure of Jiang et al. describes ET from AE molecules to fluorophores covalently coupled to the peripositions of the AE nucleus.²⁵ These AE-fluorophore constructs may have been inspired by the chemiluminescent ET work of White and Roswell with hydrazide-fluorophore conjugates.²⁶

In the present studies, using easily designed and synthesized probes, 2–200 fmol of bacterial, fungal, or both types of analyte nucleic acid sequences representing environmentally relevant sequences in seawater were detected within ~1 h without the requirement for culture, enzymatic amplification, or separation of bound from nonbound probes. In conjunction with the design principles for spectral-temporal resolved chemiluminescent probes described herein, further advances in luminometer technology (e.g., broader PMT wavelength sensitivity range, high transmittance filter sets, narrow band PMTs, rapid spectral detectors used with emission deconvolution algorithms) should facilitate simultaneous differential chemiluminescence detection of three or more distinct probe-target complexes present at even lower concentrations in the near future.

EXPERIMENTAL SECTION

Materials and methods are similar to those published previously.⁸ Briefly, oligonucleotides were synthesized at Gen-Probe Incorporated on automated synthesizers, then purified, and quantified. The controlled pore glass substrates and phosphoramidites for quencher, fluorophore, nucleotide, and amino linker monomers were from commercial sources. The probe oligonucleotides were labeled through their amino groups with 9-(2,6-dibromophenoxy-carbonyl)-10-(3-succinimidyl-oxycarbonylpropyl)acridinium iodide (Chart 1), then purified, and quantified. A low light spectrograph was used to acquire images of luminescent emissions of the probes in a hybridization reagent after chemical initiation with an alkaline hydrogen peroxide solution. The images were subsequently transformed into spectrograms and smoothed. Chemiluminescent emission time courses were acquired on a Gen-Probe Incorporated LEADER HC+ Luminometer and on a luminometer modified with two PMTs for simultaneous dual wavelength detection. Solutions contained probes with or without complementary targets in hybridization reagent and were incubated at 60 °C to facilitate hybridization. Chemiluminescent emissions were initiated by sequential injections of hydrogen peroxide and Tris-HCl pH 9.0 solutions and were recorded for up to 500 s. Detailed experimental information is available in the Supporting Information.

ASSOCIATED CONTENT

Supporting Information

Additional information as noted in text. This material is available free of charge via the Internet at <http://pubs.acs.org>.

AUTHOR INFORMATION

Corresponding Author

*E-mail: ken.browne@hologic.com.

Present Addresses

^{||}School of Biosciences, Cardiff University, Park Place, Cardiff, Wales CF10 3AX, UK.

[⊥]School of Medicine, Cardiff University, Tenovus Building, Heath Park, Cardiff, Wales CF14 4XN, UK.

Notes

The authors declare the following competing financial interest(s): K.A.B. is employed by Gen-Probe Incorporated. R.C.B., I.W., and K.A.B. are inventors on patents and/or pending patent applications related to some of the technology described in this publication.

ACKNOWLEDGMENTS

M. Majlessi and the Oligonucleotide Synthesis Group at Gen-Probe Incorporated have our gratitude for their syntheses of the oligonucleotide constructs presented in this article. We additionally thank Molecular Light Technology Research Limited for supplying N-linked AE NHS ester label. The results of this project are partially based upon work supported by the Air Force Office of Scientific Research (AFOSR) under Award No. FA9550-07-1-0027 to D.D.D.

REFERENCES

- (1) Spiegelman, S.; Watson, K. F.; Kacian, D. L. *Proc. Natl. Acad. Sci. U.S.A.* **1971**, *68*, 2843–2845.
- (2) Southern, E. M. *J. Mol. Biol.* **1975**, *98*, 503–517.
- (3) Tyagi, S.; Kramer, F. R. *Nat. Biotechnol.* **1996**, *14*, 303–308.
- (4) Nelson, N. C.; Cheikh, A. B.; Matsuda, E.; Becker, M. M. *Biochemistry* **1996**, *35*, 8429–8438.
- (5) Tyagi, S.; Marras, S. A. E.; Kramer, F. R. *Nat. Biotechnol.* **2000**, *18*, 1191–1196.
- (6) Rutter, A. J.; Weeks, I.; Li, Z.; Smith, K. U.S. Patent 7,169,554, 2007.
- (7) Brown, R. C.; Li, Z.; Rutter, A. J.; Mu, X.; Weeks, O. H.; Smith, K.; Weeks, I. *Org. Biomol. Chem.* **2009**, *7*, 386–394.
- (8) Browne, K. A.; Deheyn, D. D.; El-Hiti, G. A.; Smith, K.; Weeks, I. *J. Am. Chem. Soc.* **2011**, *133*, 14637–14648.
- (9) Nelson, N. C.; Woodhead, J. S.; Weeks, I.; Cheikh, A. B. U.S. Patent 5,756,709, 1998.
- (10) Smith, K.; Li, Z.; Yang, J.-J.; Weeks, I.; Woodhead, J. S. *J. Photochem. Photobiol., A* **2000**, *132*, 181–191.
- (11) Smith, K.; Yang, J.-J.; Li, Z.; Weeks, I.; Woodhead, J. S. *J. Photochem. Photobiol., A* **2009**, *203*, 72–79.
- (12) Bagazgoitia, F. J.; García, J. L.; Diéquez, C.; Weeks, I.; Woodhead, J. S. *J. Biol. Chem.* **1988**, *263*, 121–128.
- (13) Natrajan, A.; Sharpe, D.; Wen, D. *Org. Biomol. Chem.* **2011**, *9*, 5092–5103.
- (14) McCapra, F.; Richardson, D. G.; Chang, Y. C. *Photochem. Photobiol.* **1965**, *4*, 1111–1121.
- (15) Marras, S. A. E.; Kramer, F. R.; Tyagi, S. *Nucleic Acids Res.* **2002**, *30*, e122.
- (16) Maskiewicz, R.; Sogah, D.; Bruice, T. C. *J. Am. Chem. Soc.* **1979**, *101*, 5355–5364.
- (17) Krzyński, K.; Ożóg, A.; Malecha, P.; Roshal, A. D.; Wróblewska, A.; Zadykiewicz, B.; Błażewski, J. *J. Org. Chem.* **2011**, *76*, 1072–1085.
- (18) Hung, S.-C.; Mathies, R. A.; Glazer, A. N. *Anal. Biochem.* **1997**, *252*, 78–88.
- (19) Adamczyk, M.; Moore, J. A.; Shreder, K. *Bioorg. Med. Chem. Lett.* **2002**, *12*, 395–398.
- (20) Patel, A.; Campbell, A. K. *Clin. Chem.* **1983**, *29*, 1604–1608.

- (21) Heller, M. J.; Morrison, L. E. In *Rapid Detection and Identification of Infectious Agents*; Kingsbury, D. T., Falkow, S., Eds.; Academic Press: New York, 1985; pp 245–256.
- (22) Schaap, A. P.; Akhavan, H.; Romano, L. J. *Clin. Chem.* **1989**, *35*, 1863–1864.
- (23) Zhang, S.; Yan, Y.; Bi, S. *Anal. Chem.* **2009**, *81*, 8695–8701.
- (24) Soukka, T.; Oikari, T.; Haaslahti, V. U.S. Patent 7,790,392, 2010.
- (25) Jiang, Q.; Xi, J.; Natrajan, A.; Sharpe, D.; Baumann, M.; Hilfiker, R.; Schmidt, E.; Senn, P.; Thommen, F.; Waldner, A.; Alder, A.; Law, S.-J. U.S. Patent 6,165,800, 2000.
- (26) White, E. H.; Roswell, D. F. *J. Am. Chem. Soc.* **1967**, *89*, 3944–3945.